Liquid Crystals
Publication details, including instructions for authors and subscription information:
http://www.informaworld.com/smpp/title~content=t713926090

Smectic A-cholesteric transition in a side chain cooligomer-CE1 blend. A particular confined geometry for the TGB phase?

J. M. Gilli[a]; M. Kamayé[a]
[a] UA 190, Laboratoire de Physique de la Matière Condensée, CNRS, Faculté des Sciences de Nice, Nice Cedex, France

To cite this Article Gilli, J. M. and Kamayé, M.(1992) 'Smectic A-cholesteric transition in a side chain cooligomer-CE1 blend. A particular confined geometry for the TGB phase?', Liquid Crystals, 12: 4, 545 — 560
To link to this Article: DOI: 10.1080/02678299208029092
URL: http://dx.doi.org/10.1080/02678299208029092

LIQUID CRYSTALS, 1992, VOL. 12, NO. 4, 545–560

Smectic A–cholesteric transition in a side chain cooligomer–CE1 blend A particular confined geometry for the TGB phase?

by J. M. GILLI* and M. KAMAYÉ
UA 190, Laboratoire de Physique de la Matière Condensée, CNRS,
Faculté des Sciences de Nice, 06034 Nice Cedex, France

(*Received 11 February 1992; accepted 16 April 1992*)

The blend of an industrial cooligomer side chain cholesteric material with a polar small molecule liquid crystal of reversed chirality induces a low temperature smectic A phase [1]. We present here the change in the textural characteristics at the S_A–Ch transition observed by optical microscopy between untreated glass slides: particular fingers, different from those recently described [2], are obtained for a slow increase of temperature, starting from an unperturbed spontaneous homeotropic S_A domain. These fingers, coexisting with large S_A domains, are understandable as 180° Bloch walls introducing progressively the helicity in the medium. Over a large temperature domain, these chiral fingers coexist in an apparent thermodynamic equilibrium with the normal S_A phase, suggesting the occurrence of an analogue [3, 4] of the Shubnikov superconducting phase: probably due to the presence of the glass slides, the geometry of the screw dislocations, comparable to the vortex of type 2 superconductors, is different from the recently described case [5] of the twisted grain boundary phases of the A type.

1. Introduction

The past decades have seen a rapidly growing interest in the organization of defect constituted phases. One of the earliest examples studied is the Shubnikov phase: a type 2 superconductor which in the presence of a magnetic field can exhibit a thermodynamic phase constituted of non-superconducting parallel vortices packed in a hexagonal lattice, allowing the field flux lines, excluded from the normal superconducting regions, to penetrate the medium. The geometrical simplicity of this organization (the vortex being obliged to remain parallel to the magnetic field) allowed an early understanding of the phenomenon within the framework of a Landau–Ginzburg approach [4, 5].

Our interest in the cooligomeric material used in this study started with the discovery of the original properties of the blue phases which it exhibits [6, 7]. The blue phases are also an intricate example of such defect phases with, now, a three dimensional packing of disclinations. Here also a Landau–Ginzburg (considerably more complex) approach has allowed the development of a satisfactory model which predicts the main symmetry characteristics of the lattices. The two main reasons for the increased complexity of this second case are the following:

(i) The tensorial character of the order parameter necessary for the description of the chiral nematic medium in contrast to the complex character for the superconductor.

* Author for correspondence.

(ii) The higher possible symmetry of the expelled space property (the magnetic field in the superconductor case). The latter is particularly hard to define for blue phases. Two different kinds of singularities of the normal biaxial cholesteric order parameter coexist in fact in these phases, corresponding to both uniaxial different orders existing in the core of the double twist cylinders and in the core of the disclination lattice [8].

A third kind of defect lattice phase, exhibiting an intermediate complexity between the previously described examples has been put forward by the pioneering work of de Gennes [3] developed very recently in some theoretical papers [5] and experimentally discovered at the S_A–Ch transition of particular compounds [9]. In this case, the character of the order parameter used for the Landau–Ginzburg model is a complex number as in the Shubnikov case but the space property excluded from the smectic bulk is now the twist that molecular asymmetry tends to impose at a macroscopic level. The helical axes of the expressed chirality being imposed by an intrinsic molecular property, possess now a higher degree of liberty, than the magnetic field in the Shubnikov case.

Figure 1 shows a naïve model for the organization of these twisted grain boundary (TGB) phases. Unperturbed smectic domains of slowly varying orientations are separated by complex structure twist walls, themselves being constituted of a parallel plane array of screw dislocations. As mentioned in [5], these screw dislocations of the smectic structure are probably constituted in their core by a double twist structure to be compared to that constituting the blue phase BP1–BP2 geometrical models [8]. The topological frustration relative to the simple twist cholesteric structure associated with the nature of our three dimensional euclidian space is partly removed in the core of these objects, thus allowing for a free energy gain relative to the simple helical phase in the immediate neighbourhood of this core.

In the case of the newly discovered TGB phase, the analogy of these screw dislocations with an Abrikosov vortex, strongly suggests that these double twist cylinders constitute the region of an imperfect coexistence of smectic layered order, with twist, in the same way the outlaying regions of the vortex in the Shubnikov phase constitutes the region of coexistence of superconductivity with the magnetic field: this accounts for a favourable negative energy proper to these regions, compensating the less favourable energy of the order parameter singularity in the core of the vortex.

As we can see with the following simple geometrical arguments, the previously described planar TGB structure is probably not the only possibility for building such a coexistence structure and the known low energy cost of smectic edge dislocations restricted to a core energy [10], strongly decreased in the neighbourhood of the twisted Ch phase, together with helical instability of the double twist structures [11, 12], are probably able to stabilize more complex organizations composed of associated helical screw dislocations.

As we shall see, our experimental results concern a complex blend of different molecules, resulting not only from the association of two different compounds but being also the consequence of the use of a polydisperse oligomer sample. As discussed for blue phases [13], this fact is of importance and probably makes the thermodynamic equilibrium models used in the Landau–Ginzburg frame not applicable *stricto sensu* to these systems. In fact, the first order phase transitions transposed in these inhomogeneous systems always occur through a biphase, that is a thermodynamic separation between molecular species of different affinities for the two phases surrounding the transition. This fact is of great importance for all the cases of defect built phases

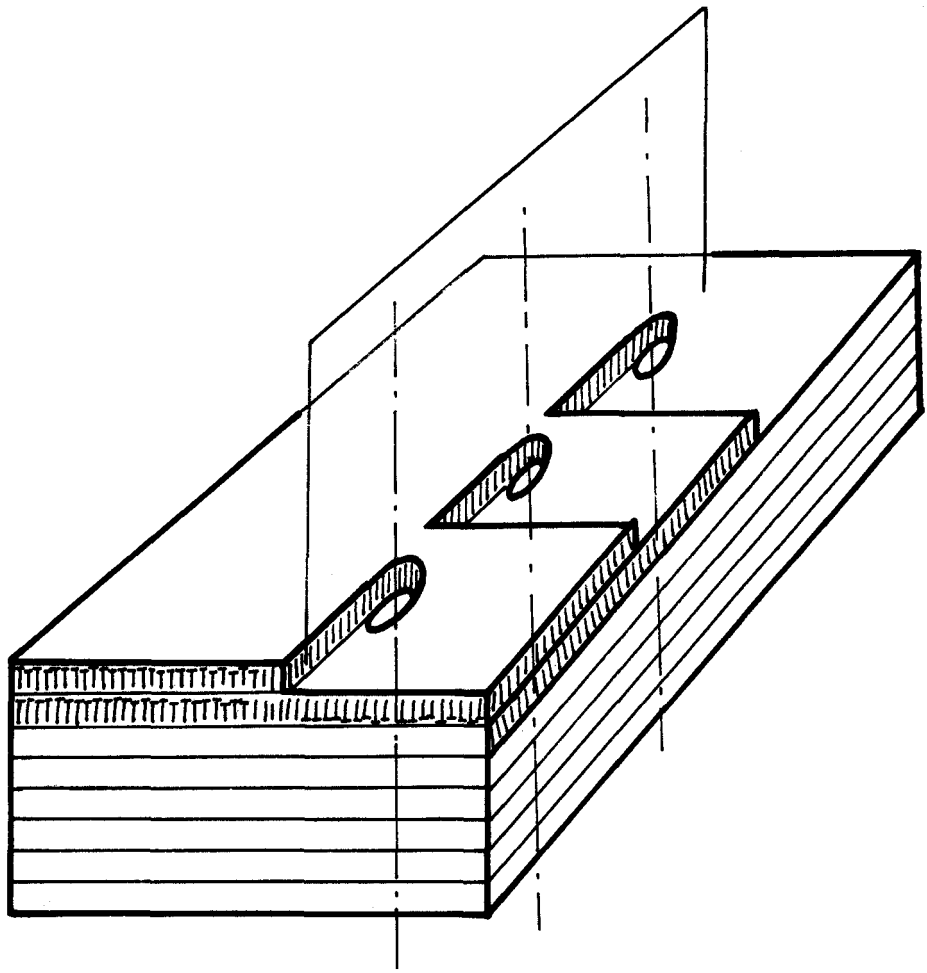

Figure 1. The twisted grain boundary of a TGBA phase, constituted of a parallel array of rank 1 screw dislocations. The resulting twist wall allows a few degrees rotation of the smectic A layer normals, from the left to the right of the drawing. In the core of these screw dislocations, the layered phase complex order parameter goes to zero. In the immediate neighbourhood of this core, the structure of the orientational order parameter is the same as for the double twist cylinder blue phase models.

discussed here, favouring a particularly enlarged temperature domain of observability for these phases (from a few tenths of degrees in pure material blue phases [8] to tens of degrees for polydisperse ones [6]): in this case, the biphasic segregation (controlled by a concentration order parameter) is probably closely associated with a periodic spatial modulation of the orientational order parameter. Another concept closely related to the appearance of these defect phases of liquid inhomogeneous media, relates them to the microemulsion domain: in contrast to the case of the generally encountered biphases (as for example nematic–isotropic) a topological reason limits the growth and coalescence of the nucleating domains and makes impossible the macroscopic separation of the two phases [13]. The case of double twist cylinders gives us a simple example of such a topological limitation of the extension of the nucleating objects. In

the case of a microemulsion composed of water, oil and a surfactant, the concept of such limited size domains comes from the optimal surface curvature associated with the conformational properties of the terminal aliphatic chains.

Finally and to relate this to the actually existing model, it is necessary to remember that the stabilization of such microemulsions, (an extended sense being given to this word), is associated with the favourable (negative) free energy of the surfaces separating the two different symmetry regions of the medium.

2. Experimental

The precise description of the two different compounds blended in this study is presented in related papers [2, 14]. Here we simply recall a few of the characteristic features of the investigated blends.

(i) The chiral cooligomer of the side chain type does not possess a true smectic phase but exhibits strong layer correlations in the whole cholesteric phase domain [1, 15]. This particular cholesteric phase can be quenched at room temperature because of the presence of a glass transition at about 50°C.

(ii) This material, named SB, is blended with the commercial compound CE1 which does not exhibit a smectic phase, but only a cholesteric over a temperature range comparable to SB. The sense of the chirality of the CE1 cholesteric phase is reversed compared to that of SB. Except probably in the immediate neighbourhood of the pure compounds, all of the blends studied exhibit a strong unwinding of the cholesteric structure with decreasing temperature, corresponding to the appearance of a large temperature domain S_A phase as demonstrated in figures 2(*a*) and (*b*) by the low angle X-ray diffraction patterns for two different concentrations. For samples with Bragg reflections in the visible region of the spectrum and introduced between planar treated glass slides, a strong unwinding of the twist is observed when the temperature decreases in the neighbourhood of the Ch–S_A transition; the normal incidence reflected colours are shifted to the red. In transmission (when no colours are observed in reflection), the birefringence progressively appears, and large fans grow when the smectic phase is produced.

(iii) We are particularly interested in the following results, for the blends incorporating 50 per cent (*w*/*w*) of both compounds. This concentration does not correspond to the racemic mixture because both compounds have different chiral units, of different rotatory power. In fact, large pitch cholesteric textures remain clearly identifiable in the upper part of the mesomorphic temperature domain. The X-ray pattern in figure 2(*b*) demonstrates the main smectic character of this blend in the bulk up to approximately 170°C, which is the temperature when the low angle peak disappears and the large pitch cholesteric phase probably appears.

3. Observation of textures between untreated glass plates

Starting at about 100°C with a 50 per cent (*w*/*w*) blend, introduced between untreated microscope glass slides, the characteristic features of the smectic A textures are easily observed; in some regions the smectic layers are nearly normal to the plates, and large, well-resolved focal conics in the fan shaped habit are observed. In other regions, the layers lay rather parallel to the slides and the striated oily streaks alternate with degenerate toric domains.

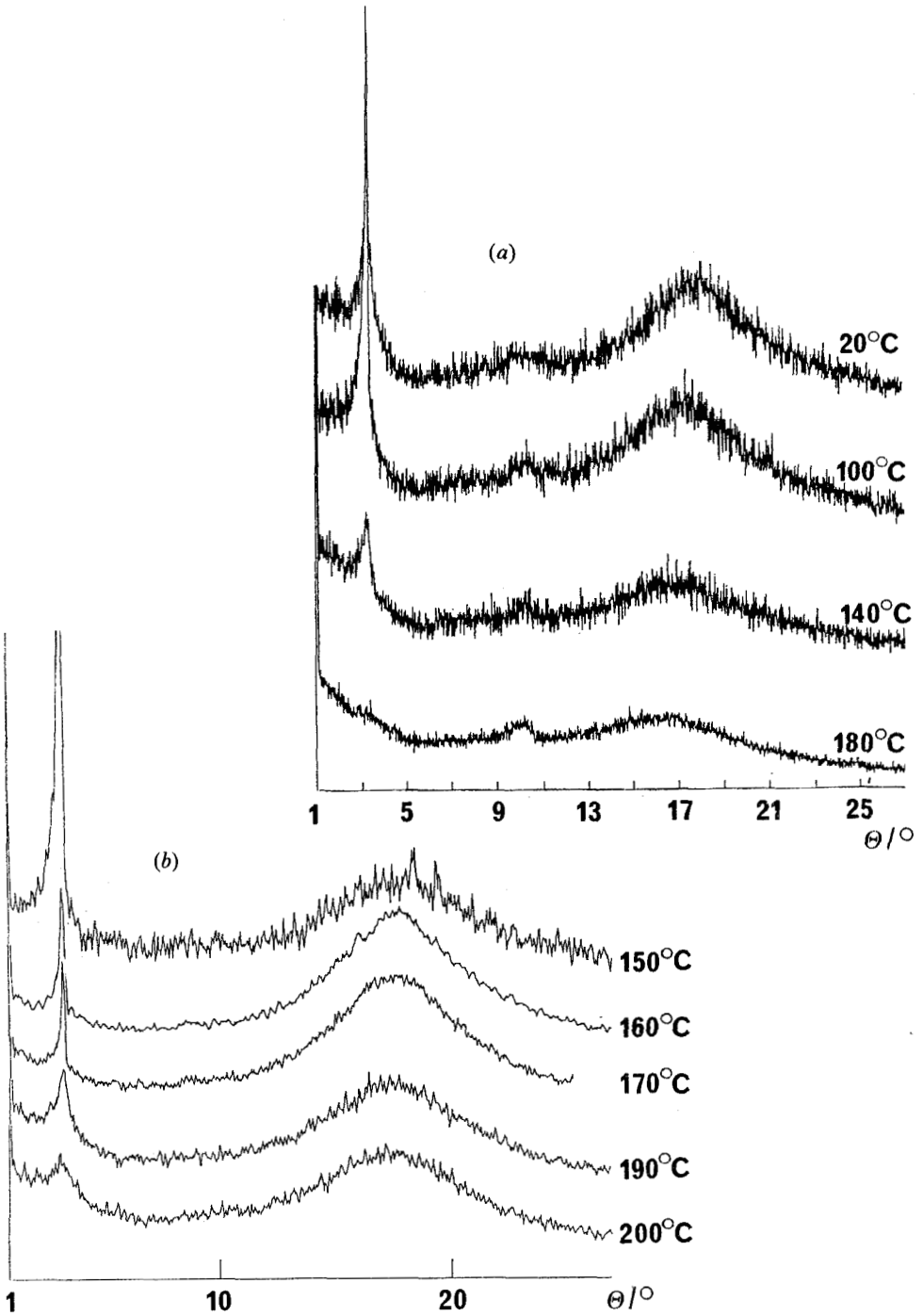

Figure 2. Successive X-ray $\theta/2\theta$ traces obtained with increasing temperature. The low angle narrow peak demonstrates the smectic A ordering of the blends at low temperatures. The angular position of this peak indicates a layer thickness of about 26 Å, in good agreement with the mesogens average molecular length. This peak widens and disappears progressively in a temperature domain depending on the blend concentration. (*a*) 5 per cent (*w*/*w*) of CE1 in SB: the smectic phase disappears at about 130°C, in good agreement with optical observations; (*b*) 50 per cent (*w*/*w*) blend shows a higher temperature S_A–Ch transition ($\approx$170°C): in this case the transition is also observable in a DSC experiment [1].

Increasing temperature favours the main parts of the sample more and more organized homeotropic texture and in the immediate neighbourhood of the upper limit of stability of the S_A phase the homeotropic textures become quasi-perfect, due to the rapid shrinking of the defects described previously. After a short annealing, a black, non-birefringent texture is observed between crossed polars. If we now again increase the temperature slowly starting from this unperturbed texture, at about 160°C, a spectacular nucleation of birefringent fingers is easily observed. If the temperature is increased fast enough, the classical fingers recently studied for a low molar mass smectic A–cholesteric transition are observed (see figure 3 (*a*)). Their structure has been identified [2] with a periodic variety of the translationally invariant cholesteric, when the decrease of the sample thickness induces the cholesteric–nematic transition [16, 17]. These correspond to a conical organization of the director, generally occurring when strong homeotropic anchoring conditions hinder the direct appearance of the lower energy normal cholesteric. These fingers could be considered only as transitional structures comparable to a growing interface instability: they are not in thermodynamic equilibrium with the smectic phase.

Figures 3 (*a*) and (*b*) remind the reader of a convenient way [16, 18] of visualizing the topology of such a finger embedded in the homeotropic matrix. The image of the director orientation is given by the mapping of the sphere S^2: a director orientation corresponds to a point on the sphere and a straight crossing of the finger, parallel to the plate is seen on the surface of the sphere as a closed curve (a circle for convenience), this curve crossing the north pole is associated with the director orientation in the homeotropic regions. The complete transverse finger organization is described by the successive opening (from the upper plate) of circles: the maximal azimuthal director angle, relative to the homeotropic organization is obtained in the middle of the plate, this trajectory t_m, corresponds to the largest circle opened on the sphere. The characteristic of the translationally invariant cholesteric is parametrized on the sphere by the $\alpha = zOM$ angle (see figure 3 (*b*)).

In the case of relatively low α, i.e. the translationally invariant cholesteric configurations studied in [2] ($\alpha < 90°$), the conical rotation of the director seen by the light propagating across the sample leads mainly, as in the planar cholesteric case, to a rotatory polarization of the light. This explains the absence of extinction observable on these fingers when the preparation is rotated between crossed polars (see figures 3 (*a*) and (*b*)): the colours observed are associated with the different rotatory powers felt by the different wavelengths of the incident light.

If we now increase the temperature very slowly from the homeotropic unperturbed domain a very different kind of finger is nucleated, presenting now a clear birefringent character. Figure 3 (*b*) shows a large domain of the plate with the coexistence of both the fingers: the observation of such coexistence being probably related to slight concentration gradients which are very difficult to avoid. If the temperature is again slowly increased (0·2°C min^{-1}) from the moment the first fingers of type 1 or 2 appeared in the observation field, the initially unperturbed homeotropic domain is progressively invaded by the fingers and we observe drastically different dynamics of progression allowing again an easy differentiation of both finger types. At a given temperature, situated at about 10°C above the temperature of appearance of the first finger T_{C1} and corresponding to the X-ray disappearance of the low angle narrow peak, a transition to the cholesteric textures is seen. In the case of the translationally invariant cholesteric first type finger, the cholesteric textures obtained reveal a mainly planar organization. For a type 2 finger, the cholesteric texture obtained preserves the alternation of clear

and dark stripes initially corresponding to the parallel finger organization (see figure 3(*c*)): the appearing cholesteric has its helix axis parallel to the plates. In fact, the moment (or temperature T_{C2}) at which these type 2 fingers associate to form a normal cholesteric probably corresponds to a slight change of the director field, mainly arising in the immediate neighbourhood of the slides.

4. Static and dynamic characteristics of the second type finger

Figures 3(*d*)–(*h*) and 5(*f*) give different examples of such observed fingers. Figure 6 shows the influence of the thickness T of the sample on the apparent thickness D of these fingers. This last parameter is rather biased, due to the probable strong cylindrical lens effect the fingers present, justified by their double twist tube model. It is clear nevertheless that the thickness of these objects depends linearly on T, their extent being a few times lower than T and that a calibration of these objects gives them a fixed radial dimension $D(T)$ which constitutes another important difference from the previously described type 1 fingers. In the latter case, the objects size is greatly influenced by the growth dynamics. The tip of these fingers (see figures 3(*d*)–(*h*)) presents obviously a singularity in the director field, as demonstrated by the strong variation of the birefringence. The helicity of the structure is seen in the vicinity of the tip when moving the microscope focus from the upper to the lower plate. It is very important to note that an apparent stability of these fingers is obtained over a large temperature range comprised between T_{C1} and T_{C2}, even on annealing for as long as one day.

Concerning now the dynamics of the propagation of these calibrated fingers, observed in a progressive increase of temperature, they obey again a behaviour very distinct from the translationally invariant cholesteric fingers. In the latter case the growth of the chirality operates via a classical dense branching mechanism (see figure 3(*a*)): to fill the space, the periodic translationally invariant cholesteric fingers branch and coalesce easily with other fingers encountered along their random progression. In type 2 fingers, however, branching is completely impossible and coalescence only occurs when two fingers having exactly the same orientation, meet by their singular tip, the connection involving the annihilation of the point defects.

Figure 3. Optical microscope textures seen in transmission between crossed polars. All of the photomicrographs presented correspond to a sample thickness between 10 and 20 μm. (*a*) An example of the type 1 finger growth, starting from the homeotropic smectic phase and increasing the temperature with a rate of about 10°C min^{-1}; (*b*) large domain of coexistence between type 1 fingers (on the right), exhibiting no birefringence, and thinner type 2 fingers (on the left): in the second case, the transmitted light intensity depends on the orientation of the fingers relative to the polars; (*c*) at low enlargement, the type 2 fingers (visible on the right) association leads to a fan shaped cholesteric texture, corresponding mainly to an orientation of the helix axis parallel to the plate; (*d*) a stronger magnification of the fingers allows the observation of their sharp tip in the upper right part of the photo: the straight finger progression is deviated by the presence of other fingers; (*e*), (*f*) successive photos of the same domain for a slow temperature increase (0·2°C min^{-1}): in the left hand bottom part of the photos, precursors of the type 2 fingers are seen around an air bubble. An isolated type 2 finger is seen in the central part, undergoing a bending instability and it transforms into a double finger such as that seen in the extreme upper part of the photos. In the right part, the large fingers observed correspond to the association of four such type 2 fingers; (*g*) the multiple association of the elementary type 2 fingers is seen here at stronger magnification; (*h*) for a low temperature increase type 2 fingers can also associate in the way observed here: they undergo a parallel straight progression: the singular tips are observable in the left hand part of the photo.

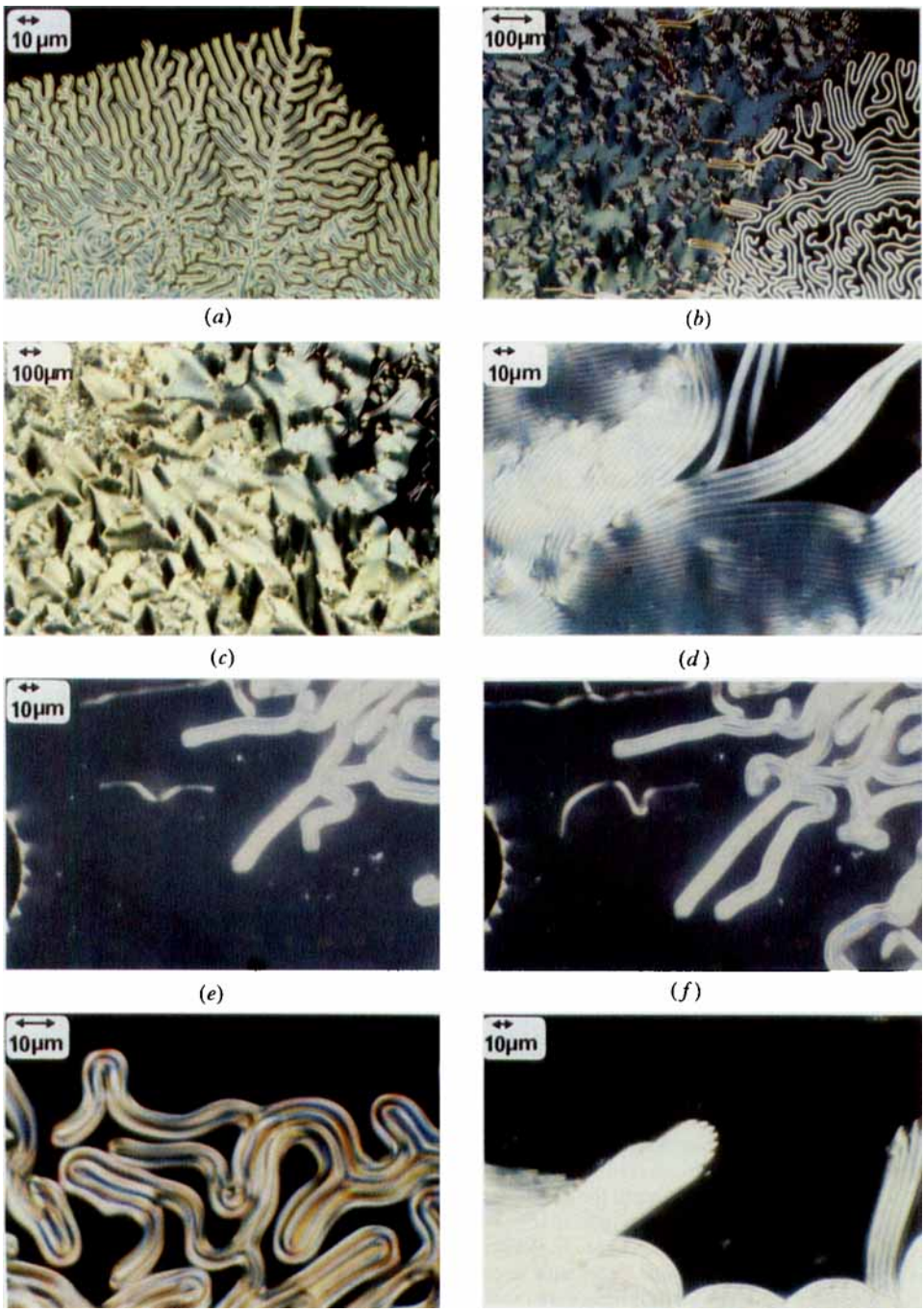

Figure 3.

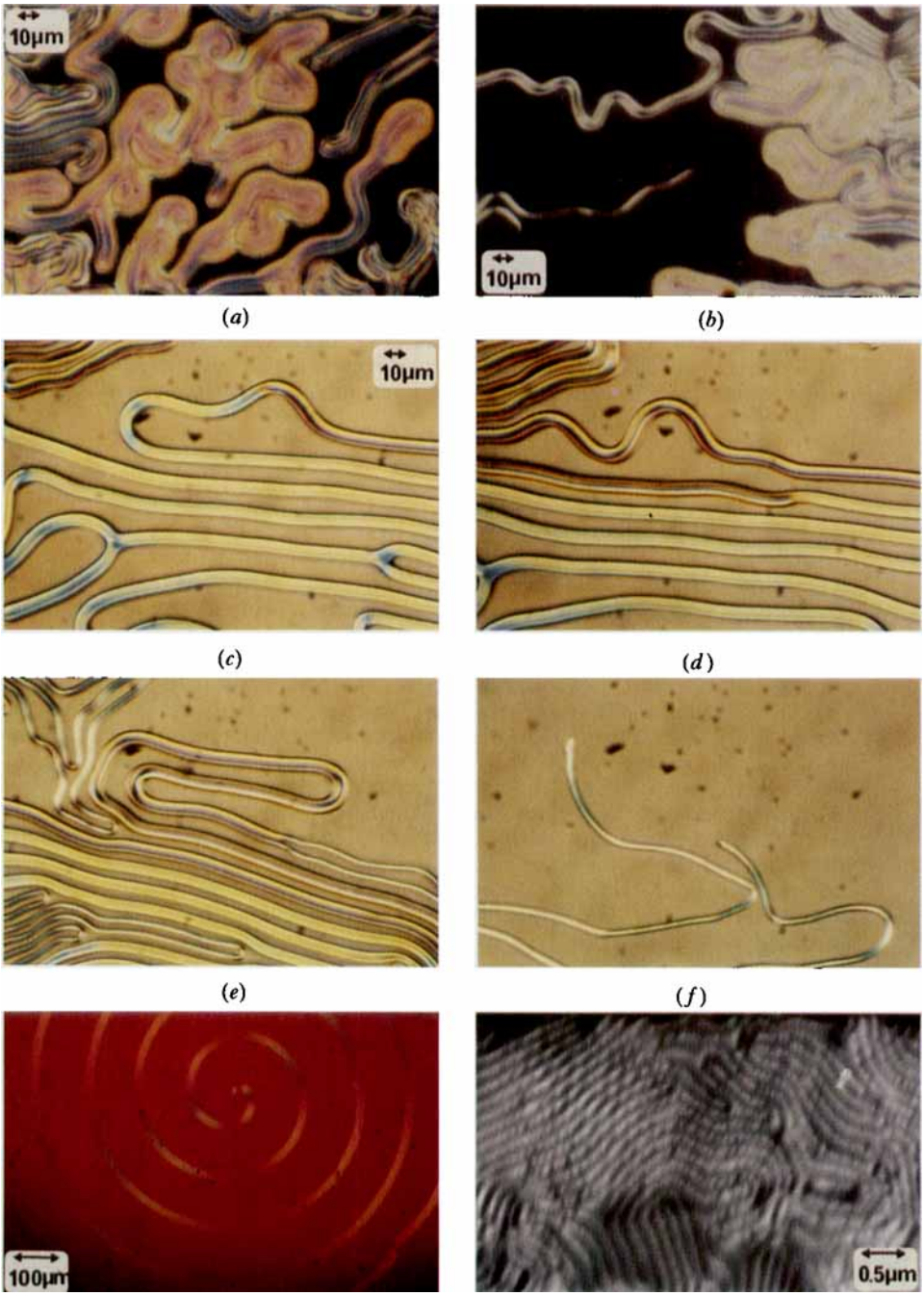

(a) (b) (c) (d) (e) (f) (g) (h)

Figure 5.

Figure 5. Photomicrographs (*a*) to (*g*) correspond to a sample thickness between 10 and 20 μm. (*a*),(*b*) Between crossed polars, a fast increase of the temperature, starting from a type 2 finger texture, allows the observation of the transformation of these latter fingers in the translationally invariant cholesteric organization: the colours observed in the central part of (*a*) and in the right hand part of (*b*) are characteristic of type 1 fingers; (*c*),(*d*) the same region observed at different times, for the same temperature: the polars have been uncrossed (as in (*e*),(*f*)): the yellow homogeneous branching fingers correspond to the type 1 translationally invariant cholesteric situation. In the upper part of the photo, a transformation of these fingers is seen: a dark region in the central part of the finger propagates at constant temperature; (*e*),(*f*) a second transformation is observed: leading to the separation of the type 1 finger into two type 2 ones as seen in the right hand part of (*e*), and in (*f*), this last type corresponding to a neighbouring region; (*g*) between crossed polars and adding a waveplate, when an AC field of particular frequency is applied normal to the plates, the fingers nucleation is replaced, in the same system, by impressive rotating archimedian spirals. (*h*) The electron microscopy transmission textures obtained by direct observation of room temperature quenched pure SB samples, reveals the presence of particular domains. These domains coexisting with normal cholesteric and blue phase 1 (not visible here) are understandable as a parallel array of double twist tubes, with random orientation relative to the cut plane and transformable in the normal cholesteric structure (in the lower part of the photo).

Figure 4. (*a*),(*b*) A useful way of visualizing the director orientation in the cross-section of a chiral finger embedded in an unperturbed homeotropic matrix [16, 18]: the director orientations corresponding to the successive trajectories t from the upper to the lower plate (*a*) are projected on the sphere S^2 (*b*), the plate normal direction corresponding to the north pole of this sphere. These successive trajectories t correspond, on the sphere, to a continuous family of circles, opened from the north pole, up to the greatest circle (associated with the middle plate t_m trajectory), and again shrunk back to the north pole. The particular translationally invariant cholesteric configuration obtained is parametrized by the angle $\alpha = z\mathrm{OM}$, M being the centre of the largest opened circle. (*c*),(*d*) Compared to the translationally invariant cholesteric situation described in [16, 18] a higher deformation of the director is imposed relative to the unperturbed homeotropic state; (*c*) the successive opened circles cross now the south pole and are shrunk to the north pole on the left side of the figure 3 (*c*): in this case, the trajectory in the middle plate corresponds to a 180° (equivalent to 0°) α angle, and to an unperturbed homeotropic situation as seen in 3 (*f*); (*d*) the lower half of the finger is described by the opposite circles succession and is described here by the circles centre trajectory. (*e*) A particular translationally invariant cholesteric director field corresponding to an angle α of 43° from [12] with the nail representation: the possibility of type 1 fingers to split into two separated cells each containing a $+1, -1$ non-singular line defect is yet observable here. (*f*) Figures (*c*) and (*d*) have shown the possibility of a continuous transform of a translationally invariant cholesteric director field into such a symmetric up–down separation of the finger. (*g*) This separation is obviously able to bring to the transverse splitting of the initial type 1 finger into two type 2 fingers. (*h*),(*i*) Models of the director field represented with the nail convention in a cross section of the finger; (*h*) the translationally invariant cholesteric situation of figure 3 (*e*) strongly suggests that each separated half cell constituting the type 2 fingers could contain associated $+1, -1$ non-singular line defects whose reassociation allows the recovery of the unperturbed homeotropic situation if the temperature is decreased; (*i*) in fact, the director field of type 2 fingers is probably closer to the more symmetric situation described here, corresponding to the splitting of the -1 defect into two singular $-1/2$ lines: the absence of anchoring treatment at the glass surface probably allows the singular lines (see here as white triangles) to become virtual, by their escape from the sample. (*j*) Corresponding to the non-singular director field situation of figure 3 (*i*), the layers are shown here in the outer part of the double twist cylinder: edge dislocations parallel to the finger axis are necessary to eliminate the variation of the layer thickness.

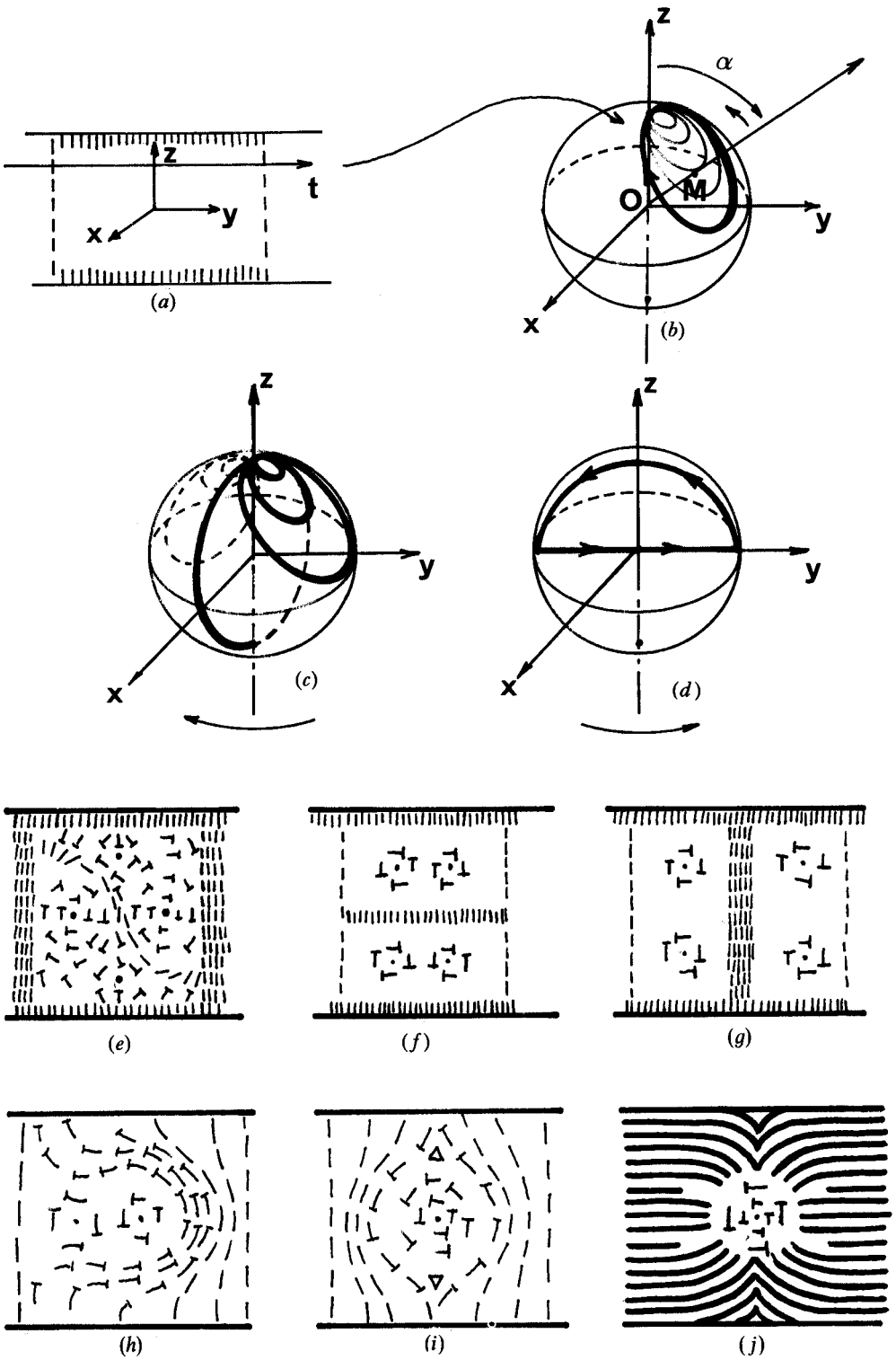

Figure 4.

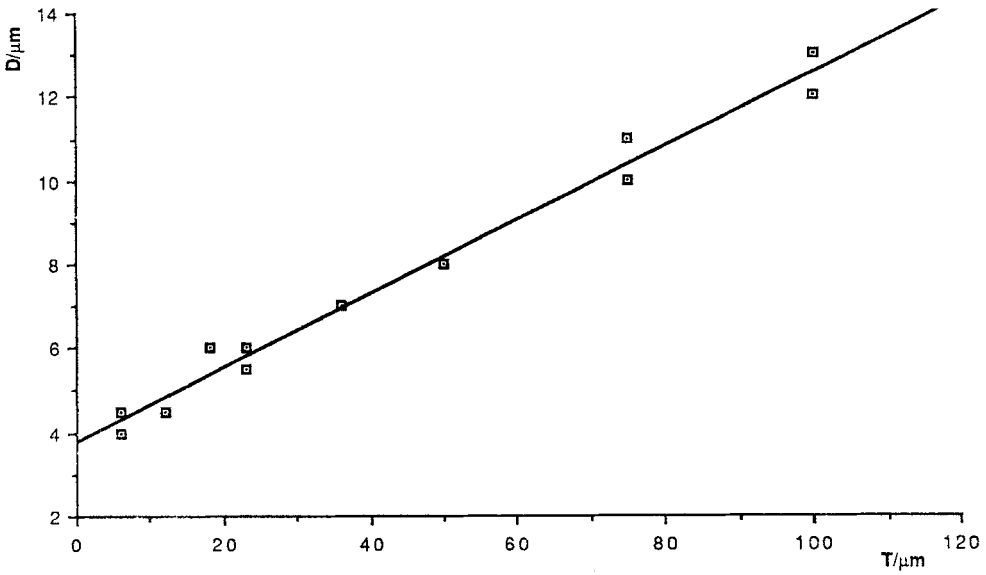

Figure 6. Variation of the apparent type 2 finger thickness D, versus the distance T separating the top and bottom glass plates.

Depending probably on the increasing rate of temperature, concentration and other factors, different processes of space filling are observable in our experiments:

(i) if the temperature increase is sufficiently slow the process mainly involves a straight progression of the finger associated with the displacement of the point defect (see figures 3 (*d*) and (*h*)). Obviously, at a certain stage, the progression of the finger considered is limited by the presence of other fingers and the observation of such events gives the impression of an impact between worms: the blind worm arriving on the lateral part of another worm is deviated and obliged to follow the direction of the second one (see figure 3 (*d*)), or it is bounded back as in an elastic impact (see figure 5 (*f*)). In some rare cases the first finger can cross the second one giving the clear impression of the superposition of the two structures in the bulk of the sample. It is necessary to remember here that the reorganization arising in all of these phenomena probably involves only rotational motions excluding group translational motions of the centres of gravity. In some cases an important number of such straight fingers associate in a related parallel progression (see figure 3 (*h*));

(ii) when the phenomenon of nucleation is more strongly activated, the motion of the fingers is no longer straight. The finger exhibits an instability and its axis takes now a spatially oscillating form. A higher bent region develops and constitutes now the extremity of a double second type of fingers as seen in figures 3 (*e*)–(*g*) and 5 (*b*). This process allows a rapid filling of the sample plane (in a manner somewhere comparable to the first steps of the Peano mathematical curves). This process is again successively repeated on the double finger formed which in its turn oscillates spatially and forms again a new multiple finger constituted of an even number of elementary elements closely packed. In fact, this successive process can be understood as an alternative to the impossibility of branching for the single fingers of the second type.

5. Transformations between type 1 and type 2 fingers

When the heating rate is increased rapidly starting from a texture exhibiting only type 2 fingers, a transformation becomes observable between the multiple fingers into those of the first type (see figures 5 (*a*) and (*b*)). But this transformation is never observed starting from a single finger of type 2. In some cases, the isolated finger initiates only a spatial oscillation and the bent region that would form a double finger, immediately gives rise to a first type finger of approximate thickness double that presented by the isolated type 2 finger. These phenomena are in this case operating at a very fast rate, making difficult their detailed description.

For the reverse transformation, the situation is considerably slower and easier to study accurately: starting from type 1 fingers, obtained by the application of a rapid enough temperature increase, this increase is now stopped at a temperature between T_{C1} and T_{C2} and they are now observed at this constant temperature. Figures 5 (*c*)–(*e*) show the transformation which arises with a very slow kinetic: the initial translationally invariant cholesteric organized finger is easily recognized by the homogeneity of its internal aspect. The photos have been taken between uncrossed polars to avoid the excessive contrast obtained in the crossed polars case. An initial transformation is visible in figures 5 (*c*) and (*d*) a dark domain deviating the light appears in the central part of the finger, by a slow progression along the axis of the finger. In a second step, this central part takes the same non-birefringent aspect as the smectic unperturbed region and the first type finger divides into two separate type 2 fingers (see figures 5 (*e*) and (*f*).

6. A possible model for these fingers

The projection of the director onto the surface of a sphere provides a useful tool with which to visualize the director field in a cross-section perpendicular to the finger. The translationally invariant cholesteric finger corresponds to the successive opening of circles from the north pole, up to a circle defining the angle α, and followed by the reclosing of the circles up to the north pole point, without having crossed the south pole. It is now possible to imagine a different process on the sphere, being in the same way associated with the opening of circles from the north pole, but bringing α up to 180°, that is to say that after being a great circle passing both poles, the circles are shrunk into the north pole on the left half surface of the sphere (see figure 4 (*c*)). To obtain an equivalent topology with the translationally invariant cholesteric case, it is necessary to repeat again the operation in the opposite way (see figure 4 (*d*)). This is the simple demonstration of the possibility of a continuous transformation of a translationally invariant cholesteric finger into two separate symmetric cells. As seen on the nails representation of a translationally invariant cholesteric finger in [12], it is not necessary to obtain an angle α as high as 90° to discover the tendency of these fingers to split into two cells having each a double twist $+1$ and a -1 non-singular defect. The resulting models of the second type finger are given in figures 4 (*h*)–(*j*): due to the absence of anchoring conditions, and to the symmetry imposed by the slides, the -1 unfavourable defect probably splits into two virtual $-1/2$ defects at the up and down limit of the slides. It is interesting to remark that this isolated structure is identical to the repeat unit model for the cholesteric between slides (with the helix axis parallel to the slides) given in [19]. The detailed optical properties of such a structure are actually unresolved theoretically but are obviously compatible with the lens effect and the positive birefringence observed experimentally.

In the case of type 2 fingers, a question arises now: are there, as in type 1, non-equilibrium transitional structures, or a stable coexistence of chiral regions, in the bulk

of smectic domains? The experiments described previously seem to demonstrate that they constitute really a stable two dimensional array of calibrated defects whose density is controlled by the temperature as in the Shubnikov phase. This is probably true with the limitations coming from the probable biphasic nature of such a system as discussed in the Introduction.

7. Discussion

If we come back to the analogy with a type 2 superconductor, we remember that the coexistence of vortices in the bulk of the superconducting volume results from the existence of particularly interesting small regions making possible a partial penetration of the magnetic flux lines into the superconducting domain: in other words, negative energy surfaces. It we try to transpose this to the case of TGB phases, the analogue of the vortex being the screw dislocation (see figure 1) [5], it appears that the periphery of the double twist tube structure seems to be a perfect candidate in being the domain of smectic correlations and twist coexistence. For the TGB phase model, the +1 screw dislocations visible in figure 1 are straight and constitute a planar twist wall. But it is possible to build another structure with helical screw dislocations: in this case, the planar twist wall of the TGB phase takes the form of a cylindrical surface. We can use a concentric array of such cylinders to transform the classical nematic double twist tube into a smectic one (see figures 7 (*a*) and (*b*)). The proposed model of such a smectic double twist cylinder embedded in a smectic A matrix (see figure 4 (*j*)) also probably needs an associated finite density lattice of edge dislocations in the strongly distorted regions joining the unperturbed homeotropic areas to the external surface of the double twist domain. An argument in support of the probable low energy of these joining domains is the similarity they present compared to the oily streak model outer regions [10]. The latter are particularly frequent defects of the homeotropic smectic A textures even far from the transition to the nematic or isotropic phase.

A question remains open concerning now the possibility of building the considered hypothetical smectic double twist cylinder without having itself an associated array of edge dislocations. The unrealizable strong thickness variation of the layers seen in figure 7 (*b*) seems to invalidate this last hypothesis, but we have to remember that this drawing shows only one helical screw dislocation: the complete model considered here involves the association of a considerable number of such screw dislocations (of the order of the number of layers joining the cylinder that is to say 10^4 for a 20 μm thick sample). Anyhow, the energy density of the edge dislocations (or the energy associated with reasonable layer thickness variations) can be strongly lowered in the proximity of the Ch phase, and favoured by the possible spontaneous splay tendencies associated with the particular cyclic side chain cooligomer used here.

The complex objects proposed here as geometrical models for the type 2 fingers previously described are also understandable as a high rank screw dislocation composed of a large number of elementary screw-dislocation-vortices intertwined as in a rope. This macro-vortex, macro-dislocation is also a 180° Bloch wall as proposed

Figure 7. (*a*) Concentric cylindrical twist walls separating different chiral smectic regions: inside each region, the layer surface adopts a helicoid shape; (*b*) each cylindrical twist wall of (*a*) is comparable to the situation drawn in figure 1, a helical shape being given to the screw dislocation constituting them. The cylindrical wall drawn here is built with a single dislocation: in the model proposed for the type 2 finger core, a considerable number of such dislocations, and concentric twist walls, are needed to avoid the strong layer thickness variation of our naïve figure.

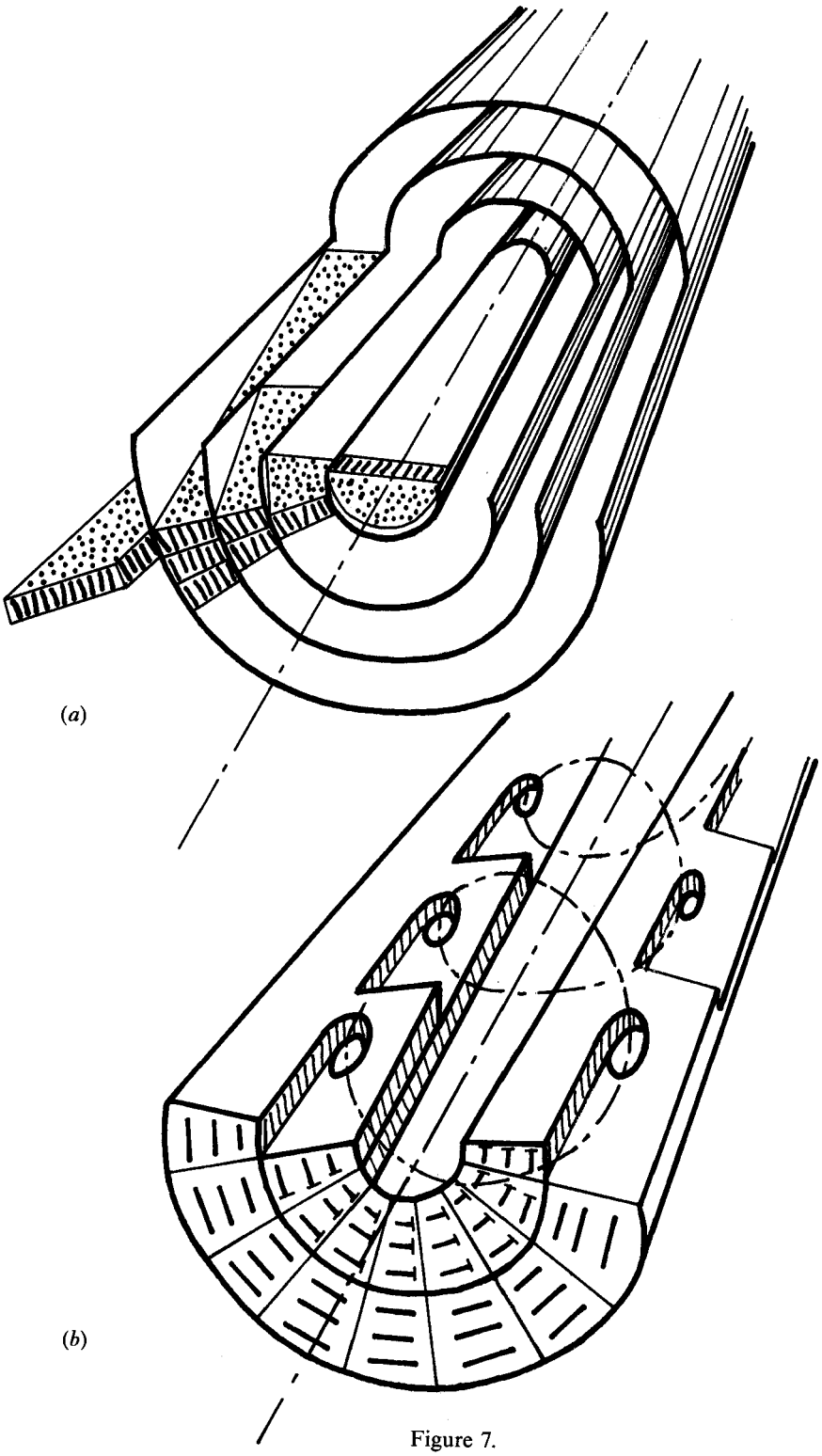

Figure 7.

elsewhere [14]: in this work, an AC field was applied to a cell similar to that of this study and type 2 finger nucleation was replaced by the formation of a quasi-perfect rotating archimedian spiral (see figure 5 (*g*)).

Compared to the TGB model of figure 1 allowing a few decrees rotation between the left and right smectic domains, the model given here changes only by the considerably higher 180° angle of the twist wall obtained.

In conclusion, we can ask the question as to the possibility of such a 180° twist wall structure in the bulk of a sample: the transmission electron micrography obtained with a cut of pure SB quenched at room temperature [7] (see figure 5 (*h*)), shows an unusual double striated structure in the neighbourhood of normal alternating clear and dark cholesteric quenched textures: this half-pitch double periodicity can probably be understood as the volume transposition of the slide confined phase described in this work. In the same quenching conditions, blue phase 1 domains have been observed in other regions of the sample [7] and a close structural relation between both defect phases exists probably with this material.

We are grateful to Y. Bin, P. Mariani and F. Rustichelli from the Laboratorio di Fisica Medica of the University of Ancona, Italy, in collaboration with whom the X-ray experiments were carried out, and to F. H. Kreuzer from Wacker Chemie for furnishing the cooligomer samples.

References

[1] GILLI, J. M., and KAMAYÉ, M., 1992, *Liq. Crystals*, **11**, 569.
[2] OSWALD, P., BECHHOEFER, J., LIBCHABER, A., and LEQUEUX, F., 1987, *Phys. Rev.* A, **36**, 5832.
[3] DE GENNES, P. G., 1972, *Solid St. Commun.*, **10**, 753.
[4] General references on superconductors: LYNTON, E. A., 1964, *Superconductivity*, 2nd edition (Methuen); 1969, *Superconductivity*, edited by R. D. Parks (M. Dekker); 1990, *Superfluidity and Superconductivity*, 3rd edition, edited by D. R. Tilley and J. Tilley (IOP Publishing Ltd).
[5] RENN, S. R., and LUBENSKY, T. C., 1988, *Phys. Rev.* A, **38**, 2132. LUBENSKY, T. C., and RENN, S. R., 1990, *Phys. Rev.* A, **41**, 4392. RENN, S. R., and LUBENSKY, T. C., 1991, *Molec. Crystals liq. Crystals* (to be published).
[6] GILLI, J. M., KAYAMÉ, M., and SIXOU, P., 1989, *J. Phys., Paris*, **50**, 2911.
[7] GILLI, J. M., KAMAYÉ, M., and SIXOU, P., 1991, *Molec. Crystals liq. Crystals*, **199**, 79.
[8] WRIGHT, D. C., and MERMIN, N. D., 1989, *Rev. mod. Phys.*, **61**, 385.
[9] LAVRENTOVICH, O. D., NASTISHIN, YU. A., KULISHOV, V. I., NARKEVITCH, YU. S., TOLOCHKO, A. S., and SHIANOVSKII, S. V., 1990, *Europhysics Lett.*, **13**, 313.
[10] KLEMAN, M., 1977, *Points. Lignes. Parois* (Les editions de physique); 1989, *Rep. Prog. Phys.*, **52**, 555.
[11] LEQUEUX, F., and KLEMAN, M., 1988, *J. Phys., Paris*, **49**, 845.
[12] LEQUEUX, F., 1988, Ph.D. Thesis, Université de Paris Sud.
[13] GILLI, J. M., KAMAYÉ, M., and SIXOU, P., 1990, *J. Phys., Paris, Colloque*, **23**, 51.
[14] GILLI, J. M., and KAMAYÉ, M., 1992, *Liq. Crystals*, **11**, 791.
[15] BUNNING, T. J., KLEI, H. E., SAMULSKI, E. T., CRANE, R. L., and LINVILLE, R. J., 1991, *Liq. Crystals*, **10**, 445.
[16] RIBIERE, P., and OSWALD, P., 1990, *J. Phys., Paris*, **51**, 1703.
[17] PRESS, M. J., and ARROTT, A. S., 1976, *J. Phys., Paris*, **37**, 387.
[18] LEQUEUX, F., 1988, *J. Phys., Paris*, **49**, 967. LEQUEUX, F., OSWALD, P., and BECHHOEFER, J., 1989, *Phys. Rev.* A, **40**, 3974.
[19] CLADIS, P. E., and KLEMAN, M., 1972, *Molec. Crystals liq. Crystals*, **16**, 1.